Chapter 4

Battery Management System for Electric Drive Vehicles – Modeling, State Estimation and Balancing

Jun Xu and Binggang Cao

Additional information is available at the end of the chapter

http://dx.doi.org/10.5772/61609

Abstract

Electric-drive vehicles (EDVs) have drawn more and more attention worldwide. As one of the most important parts of EDVs, battery management systems (BMSs) manage the huge amount of battery cells in EDVs and assures their safety. To achieve these goals, researches in BMS, such as battery modeling, battery state estimation, and battery balancing have gained a new vigor. This chapter will review the existing researches and introduce several advances in these areas.

Keywords: Battery management system, battery model, state of charge, battery balancing, electric-drive vehicle

1. Introduction

Due to pollution and energy crisis, researches in electric-drive vehicles (EDVs), including battery electric vehicle (BEV), hybrid electric vehicle (HEV), and plug-in hybrid electric vehicle (PHEV), have soared worldwide. Considered as the main power of EDVs, battery technology has drawn more and more attention [1-7]. Batteries used in EDVs should not be overcharged or over-discharged to avoid damaging the battery, shortening the battery life, and causing fire or explosions. The battery management system (BMS), with the functions of battery modeling, battery state estimation, battery balancing, etc., is one of the key points to protect the battery and optimize the utilization of the battery in EDVs.

The main purpose of this chapter is to investigate the functions of BMSs for EDVs, researches in which have gained a new vigor. Battery modeling and state estimation are among the most popular topics for BMS, and this chapter will give a detailed introduction to these topics. Battery balancing is also very important in a BMS, considering the "Bucket Effects" for a large

amount of battery cells in a battery string. This chapter will analyze the researches in this area according to literature review and a comparative analysis will be given. Several latest research results, including battery modeling, state estimation, and battery balancing, will also be introduced in this chapter.

Firstly, battery modeling methods will be investigated, including the equivalent circuit methods, impedance methods, etc. The comparison between the proposed impedance model and the measured impedance spectra will be shown and analyzed.

Secondly, the state estimation method for the battery used in EDVs, including the state of charge (SOC) estimation, will be analyzed. And a novel adaptive proportional integral observer SOC estimation method will be proposed.

Thirdly, the battery balancing method will be analyzed and compared. The positive balancing methods and active balancing methods will be introduced. A novel balancing topology will be proposed and analyzed.

Fourthly, the experimental validation will be introduced and the results will be analyzed.

Finally, conclusions of this chapter will be given.

2. Battery modeling

As an important interpretation of an actual battery, a battery model could be used as an important reference when designing the vehicle controller and estimating the states of the battery. This section will study battery models describing the characteristics of batteries. Firstly, some existing battery models will be reviewed and analyzed. Then, an impedance battery model will be proposed according to the merits and demerits of the existing battery models.

2.1. Review of battery equivalent circuit models

The battery is an electrochemical system with strong nonlinearity. To model such a strong nonlinear system is very difficult. Some attempts have been made to evaluate the battery models for the state and parameter estimation of a li-ion battery, such as electrochemical models and equivalent circuit models. Electrochemical models take advantage of electrochemical properties of the battery, and this method is relatively too complex for engineering, though it is relatively accurate. Thus, equivalent circuit models is very popular in practical applications, and several equivalent circuit models have been widely used, such as the Rint Model [8-10], the first order RC model [10-12], the second order RC model [10, 13], etc.

2.1.1. The rint model

The Rint model [8] takes advantage of an ideal voltage source V_{oc} as the open circuit voltage (OCV) of the battery. Meanwhile, a resistor R_1 is utilized to interpret the inner resistance of the

http://dx.doi.org/10.5772/61609

battery. $V_{oc}$and R_1 are both functions of SOC, temperature, and so forth and will vary with these parameters. The equivalent circuit of the Rint model is as follows:

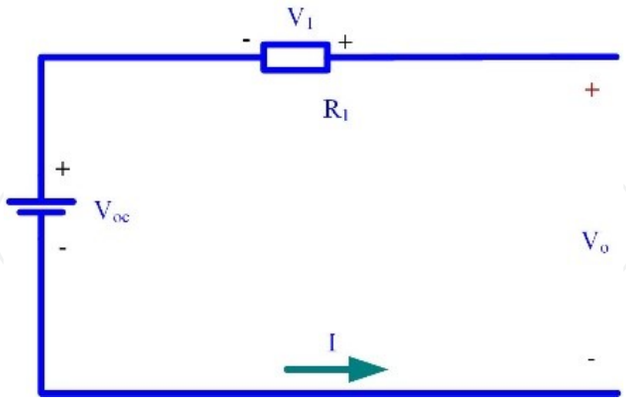

Figure 1. The equivalent circuit for Rint battery model.

In Figure 1, V_1 is used to denote the voltage between terminals of R_1, V_o the voltage of the terminals of the battery, I the current of the battery. In this chapter, the current is assumed to be positive when the battery is charging, while negative when discharging.

According to the circuit theory, following equation could be obtained:

$$V_o = V_{oc} + R_1 I \tag{1}$$

2.1.2. The RC model

The RC model was proposed by the National Renewable Energy Laboratory (NREL), which has already been utilized in the automobile simulation software Advisor [8, 14]. The RC model consists of two capacitors and three resistors. The capacitance of C_c is relatively small to interpret the surface effects of the battery. Meanwhile, the capacitance of C_b is relatively big to interpret the ampere capacity of the battery. The equivalent circuit for the RC model is shown as follows:

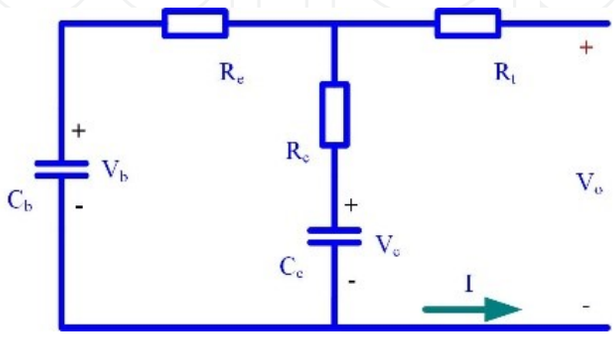

Figure 2. The equivalent circuit for the RC battery model.

Similarly, the mathematical relationship could be obtained as follows:

$$\begin{cases} \dot{V}_b = \dfrac{-1}{C_b\left(R_e + R_c\right)} V_b + \dfrac{1}{C_b\left(R_e + R_c\right)} V_c + \dfrac{R_c}{C_b\left(R_e + R_c\right)} I \\ \dot{V}_c = \dfrac{1}{C_c\left(R_e + R_c\right)} V_b + \dfrac{-1}{C_c\left(R_e + R_c\right)} V_c + \dfrac{R_e}{C_c\left(R_e + R_c\right)} I \end{cases} \tag{2}$$

$$V_o = \frac{R_c}{R_e + R_c} V_b + \frac{R_e}{R_e + R_c} V_c + \left(R_t + \frac{R_e R_c}{R_e + R_c} \right) I \tag{3}$$

where $\dot{V}_b$ and $\dot{V}_c$ means derivation of V_b and V_c respectively.

2.1.3. The first order model

The first order model [9, 15] is realized by adding a parallel RC network to the Rint model, that's why it is called first order model. The added parallel RC network is used to interpret the dynamic response of the battery. The equivalent circuit of the first order model is shown in Figure 3.

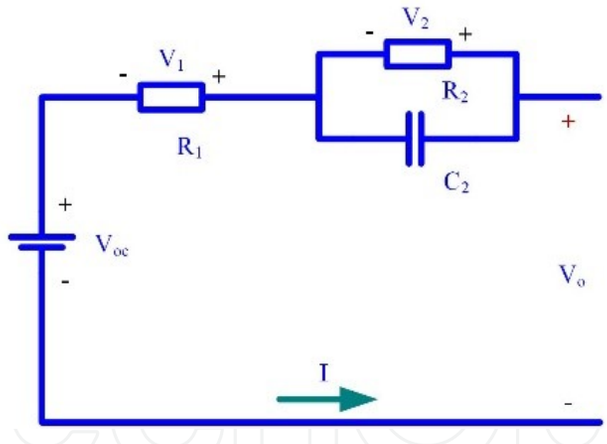

Figure 3. The equivalent circuit for the first order RC battery model.

Four parts could be included in the first order model: the OCV V_{oc}, the inner resistance R_1, the polarization resistance R_2, and the polarization capacitance C_2. $V_2$is used to denote the voltage over the parallel RC network. The mathematical relationship is as follows:

$$\begin{cases} \dot{V}_2 = -\dfrac{1}{R_2 C_2} V_2 + \dfrac{I}{C_2} \\ V_o = V_{oc} + V_2 + R_1 I \end{cases} \tag{4}$$

http://dx.doi.org/10.5772/61609

2.1.4. The second order model

Another parallel RC network added to the first order model forms the second order model. The resistance of the RC network R_3 is used to describe the concentration polarization, while the capacitance C_3 is used to describe the electrochemical polarization. The Second order model is shown in Figure 4 and the mathematical expression is shown in Eq. (5):

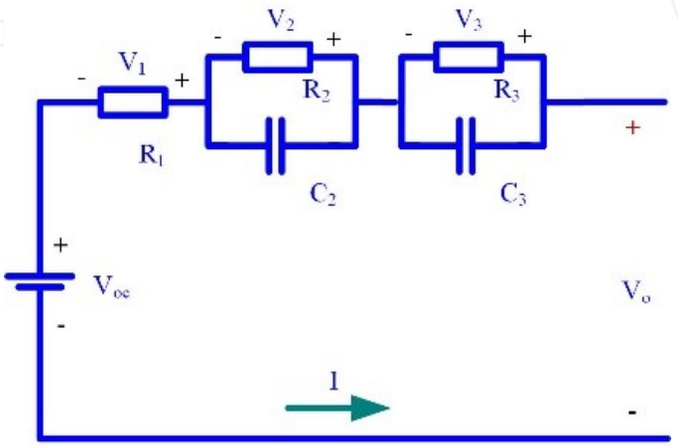

Figure 4. The equivalent circuit for the second order RC battery model.

$$\begin{cases} \dot{V}_2 = -\dfrac{1}{R_2 C_2} V_2 + \dfrac{I}{C_2} \\ \dot{V}_3 = -\dfrac{1}{R_3 C_3} V_3 + \dfrac{I}{C_3} \\ V_o = V_{oc} + V_2 + V_3 + R_1 I \end{cases} \tag{5}$$

2.2. The battery impedance model

Normally, a more accurate battery model could lead to more accurate state estimation. The models analyzed above have been widely used to estimate the states of the battery, but the problem is that they are sometimes not accurate enough to get satisfying estimation results. The electrochemical impedance spectroscopy (EIS) method is an experimental method to characterize electrochemical systems, and it is considered as one of the most accurate methods to model electrochemical systems, including li-ion batteries and supercapacitors [16-18]. However, studies have shown that the EIS method is too complex to be implemented in real time applications [19]. Besides, the impedance spectra vary with temperature, which adds difficulty to derive SOC directly from the impedance spectra. To solve this problem, an impedance model is proposed in the section [20].

2.2.1. Impedance spectroscopy test

In an EIS test, an AC current is applied to the battery, and the voltage response to the current, namely, the amplitude and the phase, is recorded. By the complex division of AC voltage by AC current, the impedance is obtained. These procedures are repeated for different frequencies, and the properties of the battery in full range frequency is obtained [21]. The dynamic behavior of batteries could be activated and recorded by the EIS test, which gives a precise impedance measurement in a wide band of frequencies. The EIS test measures the nonlinearities, as well as very slow dynamics directly, thus it is considered as a unique tool to analyze battery dynamics.

The impedance spectra of a 50% SOC battery with 3 mHz to 2.1 kHz frequency range is shown in Figure 5. Three sections can be obtained for the impedance spectra, as shown in the figure, namely, the low-frequency section, the mid-frequency section, and the high-frequency section [21].

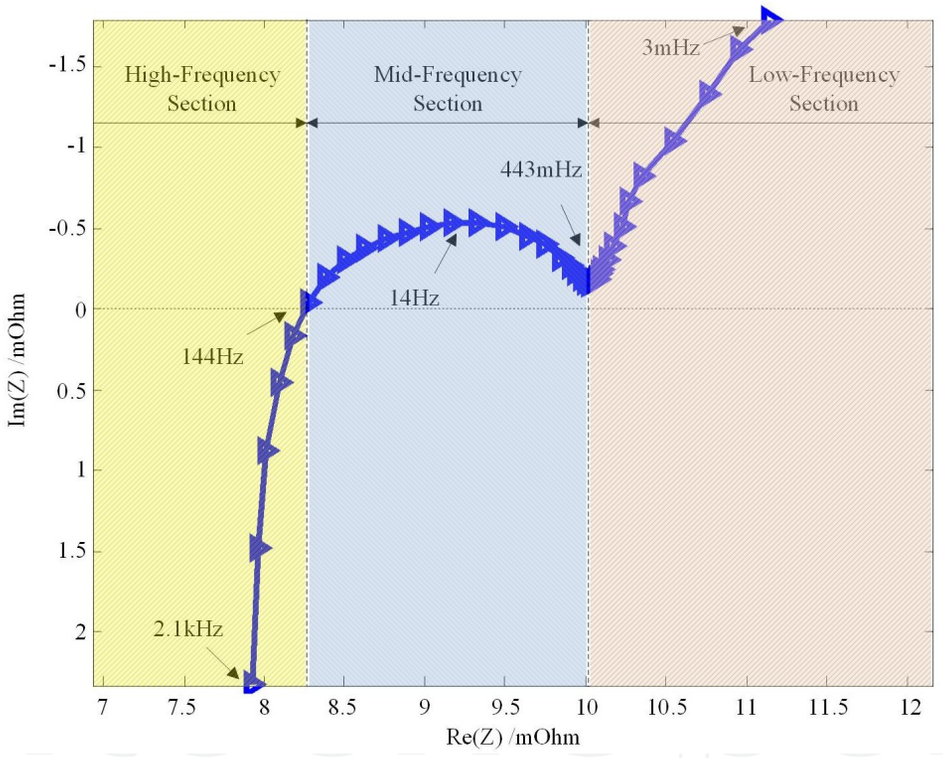

Figure 5. Impedance spectra of a Li-ion battery.

For the high-frequency section, where the frequency is larger than 144 Hz, the impedance spectra intersect with the real axis. According to the electrochemical theories (ET) and circuit theory (CT), this point could be explained by an ohmic resistance in the equivalent circuit.

When the frequency is smaller than 443 mHz, referred to as the low-frequency section, a straight line with a constant slope could be observed. This section could be expressed as a constant phase element (CPE) according to ET [18, 22, 23], which is often referred to as a Warburg element:

http://dx.doi.org/10.5772/61609

$$Z_{Warburg}(j\omega) = \sqrt{\frac{R_D}{j\omega C_D}} \coth\left(\sqrt{R_D j\omega C_D}\right) \tag{6}$$

When in the mid-frequency section (443 mHz–144 Hz), the curve looks like a depressed semicircle. According to ET and CT, this depressed semicircle could be modeled by paralleling a CPE with a resistance in an equivalent circuit, which is called a ZARC element [23]. From the analysis above, the equivalent circuit is depicted as shown in Figure 6.

In Eq. 7, V_{oc}denotes the open circuit voltage of the battery; V_1, V_2, and V_3 denote the voltage for R_1, ZARC, and Warburg respectively; V_o is the voltage output of the battery that can be measured directly from the two terminals of the battery.

$$V_o = V_{oc} + V_1 + V_2 + V_3 \tag{7}$$

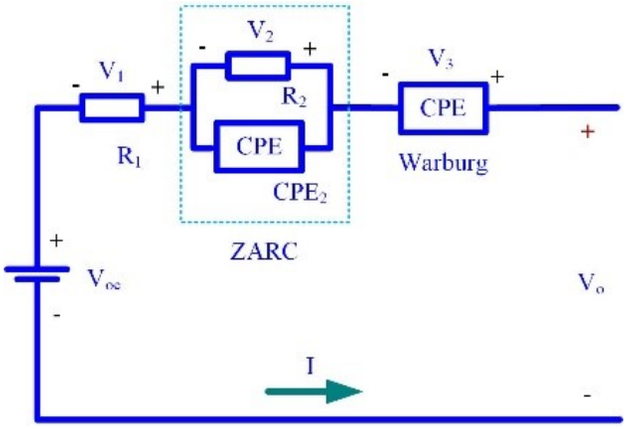

Figure 6. Equivalent circuit for the impedance model.

Then comes the problem: how to use such an impedance model with CPE in it?

2.2.2. Introduction to fractional order calculus

Considered as a natural extension of the classical integral order calculus, fractional order calculus (FOC) is becoming more and more popular. According to previous studies, most phenomena, including damp, fluid, viscoelasticity, friction, chaos, dynamic backlash, mechanical vibration, sound diffusion, etc., were considered to have fractional properties [24, 25]. Furthermore, the entire system would have fractional properties, as Machado pointed out, even if parts of it had integral properties [24, 26-28]. Based on FOC, more and more researches have been carried out to develop electrochemical models [22, 29], including lead-acid batteries, supercapacitors, li-ion batteries, fuel cells, and so on. In this section, to represent the impedance model in equations, a fractional modeling method is utilized. By this method, the impedance model can become more convenient to implement the SOC estimation of a battery.

2.2.3. Impedance model interpreted by FOC

A FOC modeling method is introduced to interpret such an element. A fractional element is given in the following equation [20, 24]:

$$Z_{fractional}(j\omega) = \frac{1}{Q(j\omega)^r} \tag{8}$$

where $r \in \mathbb{R}$ $(-1 \le r \le 1)$ is the arbitrary order of the fractional element, which can be an integer or a fraction; $Q \in \mathbb{R}$ is the coefficient. When $r = 0$, the fractional element is equivalent to a resistor; when $r = -1$, it is equivalent to an inductor; when $r = 1$, it is equivalent to a capacitor.

Furthermore, the phase of the fractional element listed in Eq. (8) is $r\pi/2$, the magnitude is $20r$ dB dec-1, and the Nyquist plot of the fractional element is a straight line. The slope of the line is a constant value $r\pi/2$, which means the fractional element is a CPE. So, a CPE can be expressed by a fractional element, which is also proved in [24]. In this way, a Warburg element can be modeled by a fractional element $Z_{warburgf}$ as shown in Eq. (9). For the relationship of fractional factor α and the slope of the curve in the low-frequency section, α can be determined by the curve slope. A Warburg element can be expressed in terms of a fractional element as follows:

$$Z_{Warburg}(j\omega) = \frac{1}{W(j\omega)^{\alpha}} \tag{9}$$

where $\alpha \in \mathbb{R}$ $(-1 \le \alpha \le 1)$ is an arbitrary number, $W \in \mathbb{R}$ is the coefficient.

Similarly, assume the equation of CPE_2 as follows:

$$Z_{CPE_2}(j\omega) = \frac{1}{C_2(j\omega)^{\beta}} \tag{10}$$

where $\beta \in \mathbb{R}$ $(0 \le \beta \le 1)$ is an arbitrary number, and $C_2 \in \mathbb{R}$ is the coefficient, especially, when $\beta = 1$,

$$Z_{CPE_2}(j\omega)|_{\beta=1} = \frac{1}{C_2(j\omega)} \tag{11}$$

CPE_2 is a capacitor and the capacitance is C_2. The paralleling CPE and resistor will form a semicircle in the Nyquist plot.

http://dx.doi.org/10.5772/61609

Figure 7 depicts the Nyquist plot where $Z_{warburgf}$ is used instead of $Z_{warburg}$ and ZARC is represented by FOC. Figure 7 shows that the fractional method can fit the measured impedance spectra well, which means the FOC impedance model can characterize the battery based on the impedance spectra analysis.

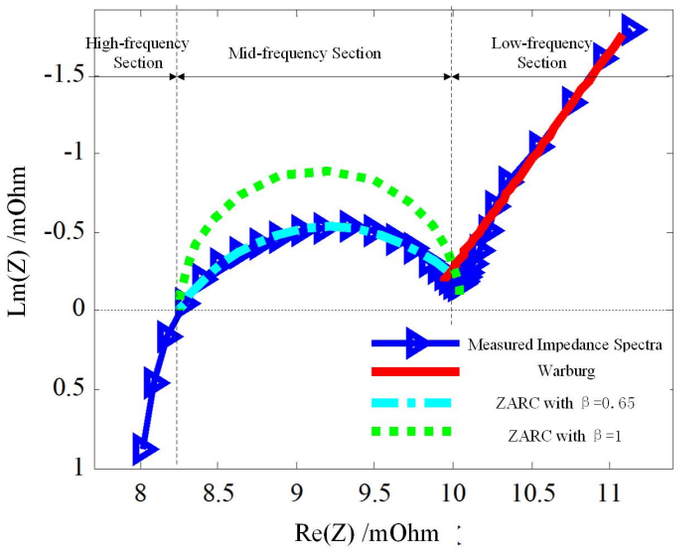

Figure 7. Comparison between measured impedance spectra and the impedance model.

3. State of charge estimation

As an essential indicator for li-ion batteries used in EDVs, SOC is a key state to estimate the driving range of an EDV. Defined as the ratio of the remaining capacity to the nominal capacity of the battery, SOC of a battery can be described as:

$$SOC = \frac{\text{Remaining Capacity}}{\text{Norminal Capacity}} \tag{12}$$

The usable SOC range could be extended if an accurate SOC can be obtained. Thus, a smaller battery pack will be able to satisfy the demand of an EDV that right now is equipped with a large battery pack. The price will be much lower and it will be a great help for market penetration of EDVs.

3.1. Existing methods for state of charge estimation

Many SOC estimation methods have been reported in previous literature, including the ampere-hour method, the OCV method, the model-based method, and so forth. The ampere-

hour method is simple and easy to implement for the calculation of battery SOC for it takes advantage of the definition of SOC. However, it needs the prior knowledge of initial SOC and suffers from accumulated errors of noise and measurement error [30, 31]. The OCV method takes advantage of the certain relationship between SOC and SOC, and is considered to be very accurate. However, to obtain the OCV needs a long rest time, and thus it is difficult be used in real-time applications [30]. Intelligent algorithms, such as fuzzy logic, artificial neural networks, and so forth, have been studied to estimate the SOC [32, 33]. Due to the powerful ability to approximate nonlinear functions, these methods can often obtain a good estimation of SOC. However, the learning process for these methods is often quite computationally demanding and complex, which becomes difficult to be applied in online applications.

Model-based SOC estimation methods are the most popular solutions [34-36]. The main methodology is to take advantage of both the voltage and the current of the battery. Measured currents will be applied to the model and the voltages will be calculated using the present and/or past states and parameters of the model. The errors between the calculated voltages and the measured voltages are applied to an algorithm to intelligently update the estimation states of the model. The Luenberger observer [37-39], the Kalman filter [40, 41], and the sliding mode observer [42-44], etc. could be used in such model-based SOC estimation methods.

Proposed by D. Luenberger [45] in 1966, the Luenberger observer is now widely used in different applications. Reference [37-39] introduced it to estimate the battery SOC and owned good results. The Kalman filter uses the entire observed input data and output data to find the minimum mean squared error estimation states of the true states of the li-ion batteries [41]. Essentially, the Kalman filter takes advantage of the prior input currents and output terminal voltages to obtain the Kalman gain. This Kalman gain is like the Luenberger gain, which feedbacks to correct the differences between the calculated states and the true states of the li-ion battery.

Reference [42] introduced the sliding mode observer to estimate the battery SOC. As indicated in the paper, the sliding mode observers inherited the robust properties in SOC estimation. It is robust under modeling uncertainties, but the chatter problem could not be ignored for this method. The block diagram of these methods is shown in Figure 8.

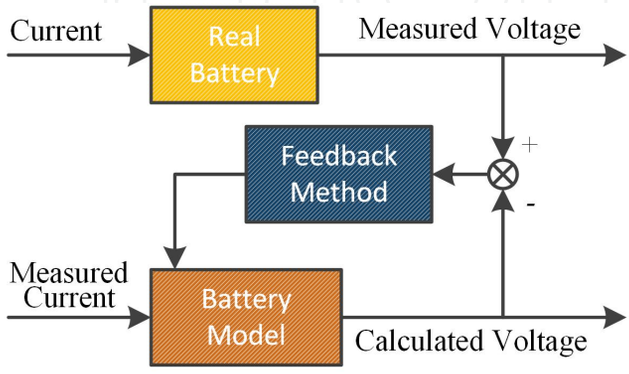

Figure 8. Block diagram of the existing SOC estimation methods.

http://dx.doi.org/10.5772/61609

3.2. The proportional integral observer SOC estimation method

By an additional integrator, the proportional integral (PI) observer is reported to be more robust with respect to modeling uncertainties [46]. Since modeling errors always exist in a battery model, the PI observer is considered to be able to improve the accuracy and estimation speed of SOC estimation. Thus, the PI observer SOC estimation method is proposed in the section. [47]

A battery model could be considered as follows (referred to as System 1):

$$\begin{cases} \dot{x} = Ax + Bu \\ y = Cx + Du \end{cases} \tag{13}$$

However, considering the modeling errors, capacity variation, and so forth, System 1 is not sufficient to model the battery. The nonlinear part should be added to the battery model, which could be described as follows (referred to as System 2) [48-50]:

$$\begin{cases} \dot{x} = Ax + Bu + Ev(x,u,t) \\ y = Cx + Du \end{cases} \tag{14}$$

where E describes the influence of the nonlinearities to the different states, and such relationships could be obtained by experiments and some "trial and error" approaches; $v(x, u, t)$ describes the nonlinearities, unknown inputs, and un-modeled dynamics of the plant and may be a nonlinear function of states, inputs, and time; $v(x, u, t)$ is referred to as disturbance.

Considering the special applications of the battery for EDVs, the disturbance could be caused by temperature, sensor noise, and so on. Taking temperature as an example, the variation rate could be very slow, and thus $\dot{v} \approx 0$ when the temperature is considered. Meanwhile, the operation temperature range for the battery is limited for the consideration of life cycle and safety. So, $v(x, u, t)$ should also be in a small range due to the influence of temperature. For the strict temperature control in EDV applications, the temperature would be stable after a short time, thus $\lim_{t\to\infty} v(x, u, t)$ exists for the influence of temperature. It is considered to be Gauss Noise with zero mean value for sensor noise. Sensor failure could also be considered to be slow changing, and thus the assumption $\dot{v} \approx 0$ could be reasonable. Actually, since the change rate is so small, the sensor drift could be neglected for a certain drive cycle of the EDV as it changes very little for a one-day drive of the vehicle. It is reasonable to assume that $\lim_{t\to\infty} v(x, u, t) = 0$ for the influence of current sensor. So it is assumed that the disturbance $v(x, u, t)$ is not state-dependent, and it is also reasonable to assume that the limitation of disturbance $v(x, u, t)$ exists.

According to the definition of the PI observer, the PI observer is designed as follows:

$$\begin{cases} \dot{\tilde{x}} = A\tilde{x} + Bu + K_p(y - \tilde{y}) + K_{i2}w \\ \dot{w} = K_{i1}(y - \tilde{y}) \end{cases} \tag{15}$$

Note that variable w is defined as the integral of the difference$(y-\tilde{y})$. Vectors $K_p \in \mathbb{R}^{2\times1}$ and $K_{i1} \in \mathbb{R}^{1\times1}$ $K_{i2} \in \mathbb{R}^{2\times1}$ are the proportional and integral gains, respectively. The design block of the PI observer is given in Figure 9.

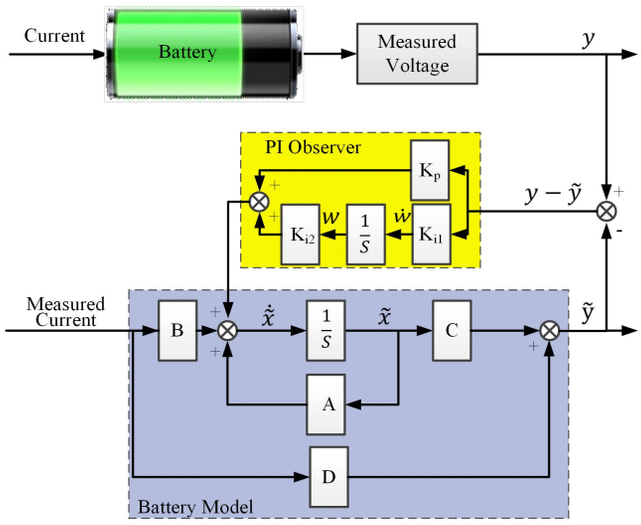

Figure 9. Block diagram of the PI observer SOC estimation method.

The unknown disturbance is considered, which would lead to modeling more accurate battery characteristics. The PI observer is applied to System 2 and when $e_x = \tilde{x} - x$, $e_v = w - v$, and $K_{i2} = E$ are assumed, the error equations could be obtained as follows:

$$\begin{cases} \dot{e}_x = Ae_x - K_p Ce_x + K_{i2}e_v \\ \dot{w} = -K_{i1}Ce_x \end{cases} \tag{16}$$

These equations could be rewritten as:

$$\begin{pmatrix} \dot{e}_x \\ \dot{w} \end{pmatrix} = \begin{bmatrix} A - K_p C & K_{i2} \\ -K_{i1}C & 0 \end{bmatrix} \begin{pmatrix} e_x \\ e_v \end{pmatrix} \tag{17}$$

So,

$$\begin{pmatrix} \dot{e}_x \\ \dot{e}_v \end{pmatrix} = A_e \begin{pmatrix} e_x \\ e_v \end{pmatrix} - \begin{bmatrix} 0 \\ I \end{bmatrix} \dot{v} \tag{18}$$

Since $\dot{v} = 0$ for the certain application as stated above, this equation could be rewritten as follows:

http://dx.doi.org/10.5772/61609

$$\begin{pmatrix} \dot{e}_x \\ \dot{e}_v \end{pmatrix} = A_e \begin{pmatrix} e_x \\ e_v \end{pmatrix} \tag{19}$$

If following matrix pair is observable, $A_e$could be arbitrarily assigned.

$$\left(\begin{bmatrix} A & E \\ 0 & 0 \end{bmatrix}, \begin{bmatrix} C & 0 \end{bmatrix} \right) \tag{20}$$

which is equivalent to:

$$rank\left\{ \begin{bmatrix} A & K_{i2} \\ C & 0 \end{bmatrix} \right\} = n + r \tag{21}$$

where r is the dimension of v, which is assumed to be 1. Since n=2 according to the battery model, the rank should be 3.

Substitute the parameters of the battery model into the matrix:

$$rank\left\{ \begin{bmatrix} A & K_{i2} \\ C & 0 \end{bmatrix} \right\} = rank\left\{ \begin{bmatrix} -\frac{1}{R_2C_2} & 0 & K_{i2_1} \\ 0 & 0 & K_{i2_2} \\ 1 & a_i & 0 \end{bmatrix} \right\} = 3 \tag{22}$$

The matrix is full rank, so the conditions are satisfied that A_e could be arbitrarily assigned.

By utilizing the pole place method or LQ method, $K_p$and K_{i1} could be selected to assure A_e is Hurwitz. Since A_e is Hurwitz, the system is convergent. Thus, when $t \to \infty$, errors will tend to be zero, which means when $t \to \infty$, $\tilde{x}$ would converge to x. Take the battery model in this chapter for example, the estimated SOC would converge to the true SOC.

4. Battery balancing

Battery technology has attracted more and more attention as stated above [51, 52]. However, single batteries could not be used widely in actual applications, since the voltage and capacity of a single battery cell is inherently low. For actual applications, such as utility energy storage in smart grids and EDVs, the battery pack is designed to be hundreds to thousands of volts to optimize the system performance. A large number of battery cells connected in series and parallel to form the battery string are necessary in such applications.

However, no two battery cells could be the same. Such differences could be internal resistance, degradation level, nominal capacity, ambient temperature, etc. These inevitable differences

among the cells in a battery string would lead to imbalance, which would cause many problems. Due to the "Bucket Effects", the actual available capacity of the battery string would dramatically decrease. Overcharge and/or overdischarge could also be potentially caused by the imbalance, which is dangerous for batteries. Battery balancing is of paramount importance to maintain the performance and enhance the cycle life.

4.1. Existing balancing topologies

Many battery balancing methods have been presented in previous studies [53-66], which could be categorized as passive balancing methods and active balancing methods. For passive balancing methods [67-69], the excess energy would be removed from high-energy cell(s) through resistors. The energy is dissipated as heat through resistors, which not only wastes electricity energy, but also increases thermal control difficulty of the battery pack. Besides, only the high-energy battery cells work in the balancing process. A large amount of energy would be wasted if most of the battery cells have higher energy than some other cells.

For active balancing methods, active switching circuits are utilized to transfer energy between cells or between the cell(s) and the battery string. Compared to passive balancing methods, wasted energy will be very little. However, to fulfill the functions stated above, more switches and associated components are needed, which would lead to increased cost and reliability concerns. The cost and reliability should be carefully considered to make active balancing more competitive, including but not limited to, reducing the components, simplifying the structure of the topology, and reducing the control complexity.

A bi-directional buck-boost converter-based balancing topology [59-61] is shown in Figure 10a, which is referred to as Topology 1. In this method, a buck-boost converter is formed to transfer energy from a high energy cell to its adjacent cell. The problem is that cells can only be balanced by their adjacent cells. More than one step will be needed if the two cells that need to be balanced have a long distance (C_1 and C_n for instance). In this case, longer time will be needed to transfer energy between these two cells to fullfil the balancing.

Figure 10b shows another widely used balancing topology [62, 63], which is referred to as Topology 2. In this topology, the primary winding of a bi-directional Flyback converter is connected to each cell while the secondary winding is connected to the battery string terminals. A cell to the battery string balancing method is formed in this method, t. cells could be balanced simultaneously since each cell owns a separate converter. The total balancing time could be dramatically reduced compared with Topology 1. However, for n cells battery string, $2n$ switches and $2n$ windings are needed. High voltage stress needs be applied to the switches in the secondary winding of the transformer. The turns-ratio of the transformer should be designed to be large enough to cover the large voltage difference between cells and battery string. These aspects would result in high costs for the system.

Another widely used balancing topology is depicted in Figure 10c [60, 64-66], which is referred to as Topology 3. Only one multi-winding transformer is utilized in this topology. n primary windings of the transformer are connected to n battery cells, respectively, and the secondary winding is connected to the battery string terminals. Only one single converter is utilized in

http://dx.doi.org/10.5772/61609

this topology compared with Topology 2. The switches used in this topology are reduced to $n + 1$. Furthermore, high voltage stress will only be applied to one switch in this topology. The secondary windings are also reduced to one. Compared with Topology 2, the cost would be dramatically reduced. However, only one cell could be balanced at a time in this topology, and it is still a string to cell balancing method. Comparing to Topology 2, these aspects lead to a longer balancing time. Besides, the converter efficiency would be almost the same since the transformer turns-ratios are the same as those of Topology 2.

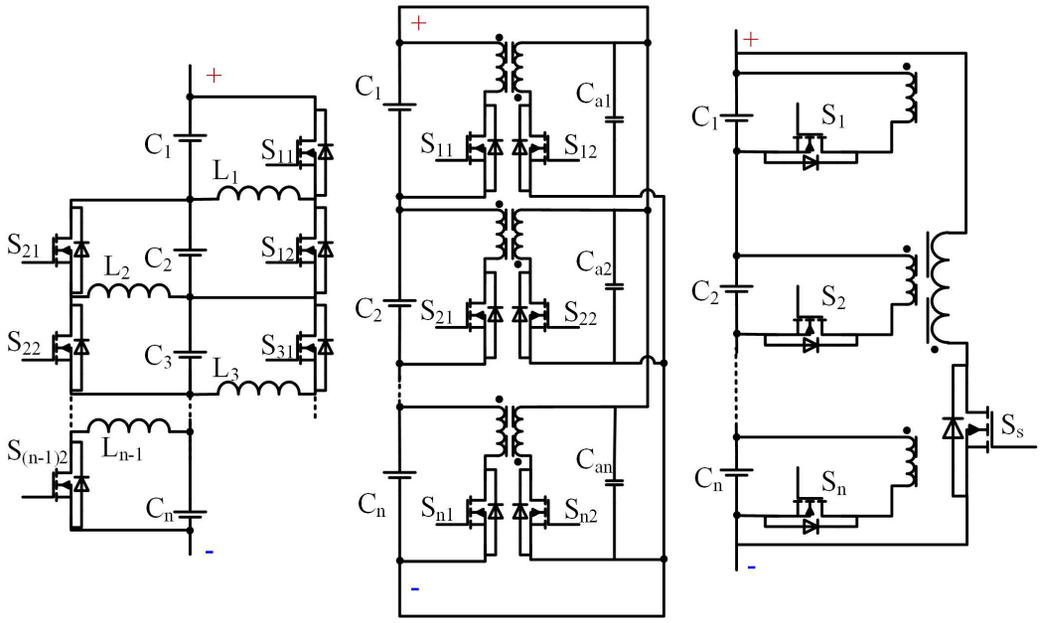

Figure 10. Active balancing topologies: (a) Topology 1, (b) Topology 2, (c) Topology 3.

4.2. The advanced cell to cell battery balancing topology

Based on the analysis of the three popular balancing topologies discussed above (as shown in Figure 11), an advanced cell to cell battery balancing topology is proposed [70]. In this topoloy, the number of switches and the number of windings are reduced. Thus, the cost will be lower and reliability will be higher due to reduced component count. Simultaneously, a much simpler control and gate drive system is needed with fewer switches. Since the topology realizes the cell to cell balancing, balancing time and complexity of the control processes will be reduced a lot. Furthermore, since the transformer turns-ratios are low, almost equals to 1, a relatively higher balancing efficiency and small size transformer could be achieved in this topology.

In Figure 11, L_1, L_2, to L_k are coupled windings, and every two cells in the string share one of such windings. For example, C_1 and C_2 share the same winding L_1. Current I is the main current applied to the battery string, while I_1, I_2,..., and I_{2k} are the balancing current for each cell, respectively. To ensure every two cells sharing a winding, the total number of cells (n) in the battery string are designed to be even ($n=2k$, $k=1, 2...$).

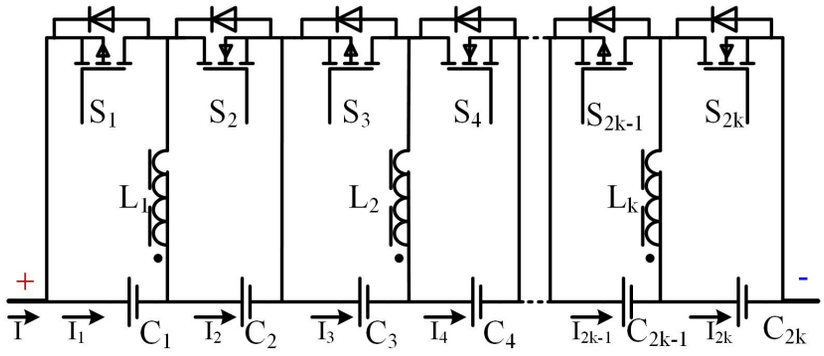

Figure 11. The proposed advanced cell to cell battery balancing topology.

In this topology, the two adjacent cells, which share one winding ($C_1$and C_2 for instance), would form a buck-boost converter similar to that of Topology 1. Meanwhile, due to the coupled windings, non-adjacent cells ($C_1$and C_4 for instance) and its windings form a Flyback converter. So balancing could be easy, no matter if the cells are adjacent or not. The cell to cell balancing method is realized and is considered to be time-saving. To compare this topology with the other above-stated topologies, the components needed for an n cell string are compared in Table 1.

	Topology 1	**Topology 2**	**Topology 3**	**Proposed Topology**
Windings	n-1	2n	n+1	n/2
Ferrite Cores	0	n	1	1
Switches	2n-2	2n	n+1	n
Switches Suffering High Voltage Stress	0	n	1	0
Balancing Type	Between Adjacent Cells	Between Cell and String	Between Cell and String	Between Arbitrary Cells

Table 1. Dear authors, please add caption

As shown in Table 1, for the proposed topology, only one switch and one winding are needed for each cell. All the switches used in the proposed topology will not suffer high voltage stress. The cost would be dramatically reduced and the controlling complexity will also be lower.

5. Experimental validation

5.1. Battery test

To learn the characteristics of the battery, different types of battery tests have been taken out in the laboratory.

http://dx.doi.org/10.5772/61609

5.1.1. Capacity test

Capacity test is firstly carried out to obtain the actual capacity of the battery.[71] The testing results are as shown in Figure 12.

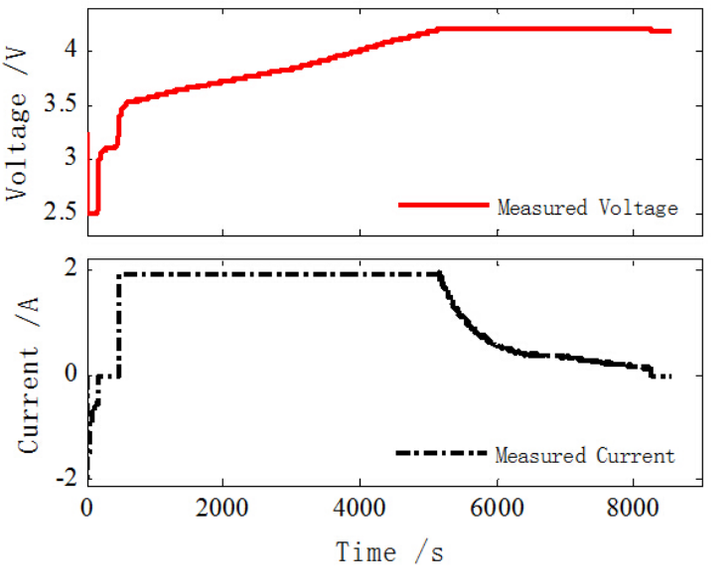

Figure 12. Testing results of the capacity test.

5.1.2. Hybrid pulse power characterization test

The Hybrid Pulse Power Characterization (HPPC) Test is intended to determine the dynamic power capability over the device's useable charge and voltage range using a test profile that incorporates both discharge and regeneration pulses. The results are as follows:

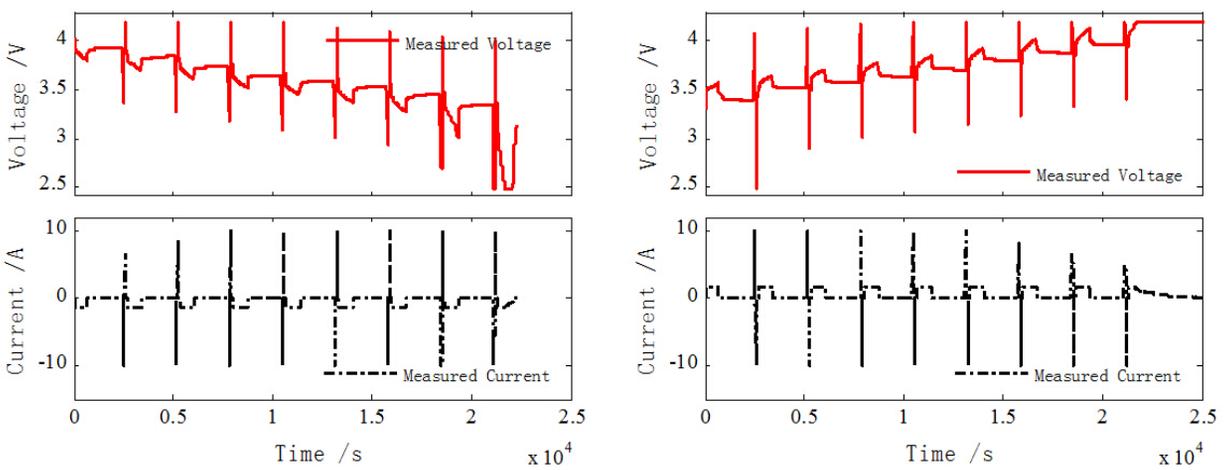

Figure 13. Testing results: (a) HPPC test when discharging; (b) HPPC test when charging.

5.1.3. Driving cycle test

UDDS and US06 drive cycles are applied to the battery. The magnitude of the current profile has been scaled down with respect to the battery features. The current profile of the UDDS drive cycle is given in Figure 14, while the testing results are shown in Figure 15.

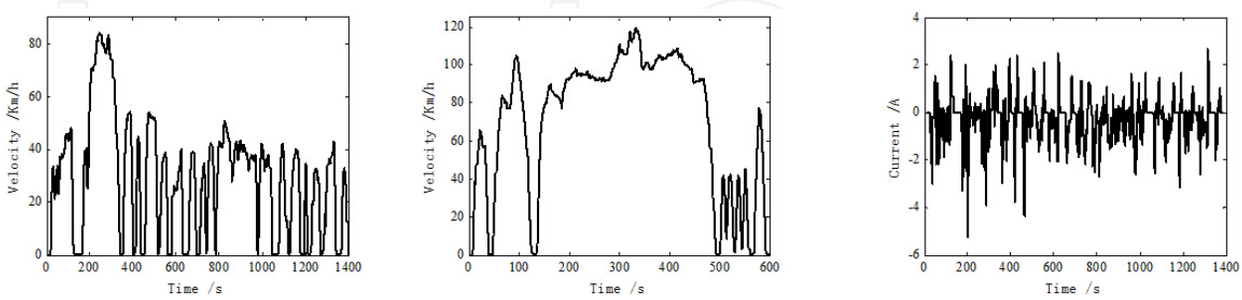

Figure 14. Different driving cycles: (a) UDDS driving cycle; (b) US06 driving cycle; (c) current profile of a UDDS driving cycle.

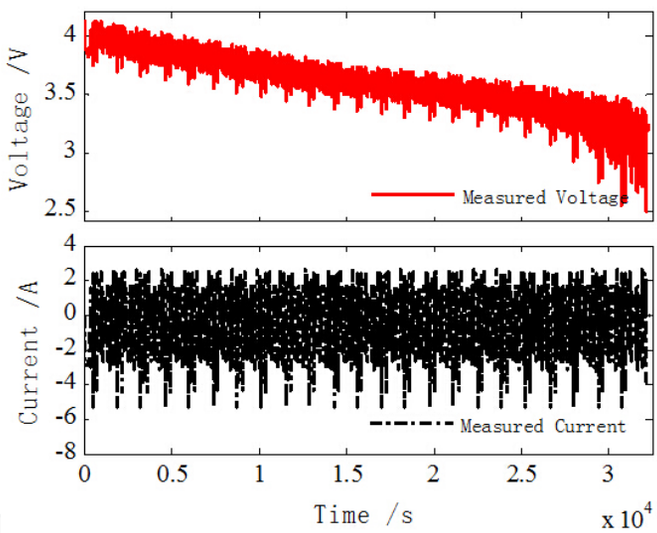

Figure 15. Testing results with UDDS driving cycles.

5.2. Experimental results and analysis

The widely used UDDS current profile is introduced to simulate the drive cycles of an EDV. The ampere counting method is utilized to calculate the reference SOC. The configuration of the battery test workbench is shown as Figure 16.

5.2.1. State estimation validation

Two cases are studied in the validation procedure. The initial SOC is assumed to be given for the SOC estimation method in the first case. The estimation results in this case are given in

http://dx.doi.org/10.5772/61609

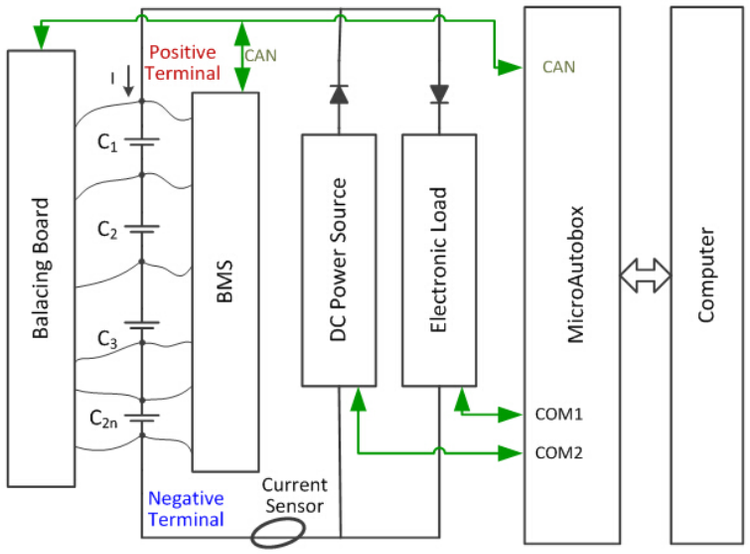

Figure 16. The configuration of the battery test workbench.

Figure 17. The SOC diverges a little in the beginning, since the model is not so accurate. Then, the estimated SOC quickly converges to and keeps on tracing the reference SOC. The results given in Figure 17 show that the SOC estimation method could estimate the SOC with small errors when the initial SOC is given.

The initial SOC is assumed to be unknown in the second case, as shown in Figure 17. In this case, the reference SOC is actually 100% but the initial SOC of the SOC estimation method is assumed to be 60%. It is clear from the figure that the estimation error is 40% at first. Then the estimation errors reduce quickly, and the estimated SOC converges to the reference SOC. After the steady state, the estimated SOC traces the reference SOC with small errors. The results indicate that the initial SOC error could be compensated by the proposed SOC estimation method and the estimated SOC will converge to the reference SOC quickly.

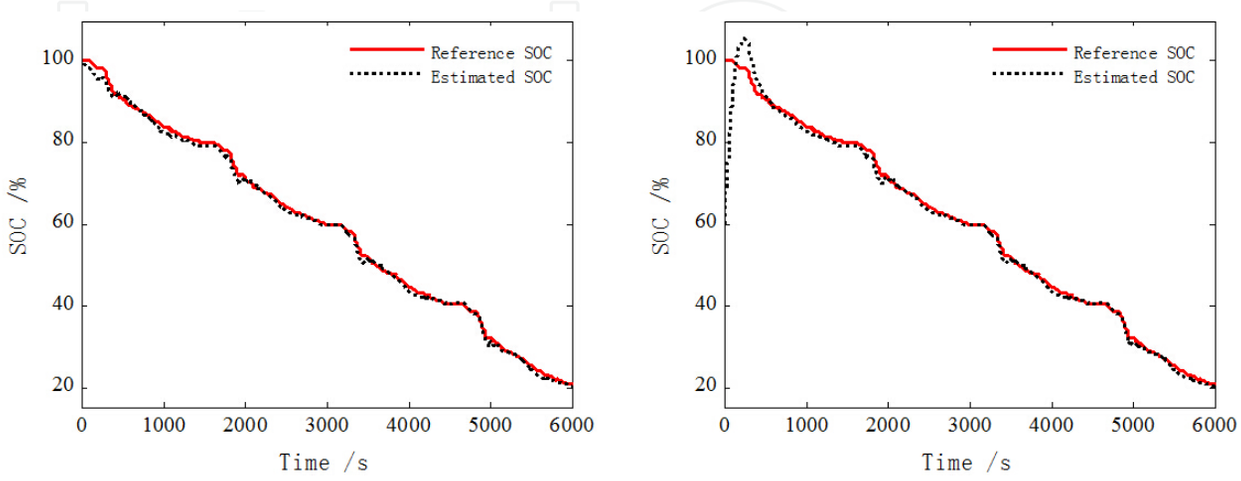

Figure 17. SOC estimation results when the initial SOC is known or unknown.

From the discussions above, it can be concluded that the SOC estimation method works well for li-ion batteries. The SOC estimation errors are small even with a simple battery model, compensating the modeling errors and modeling uncertainties.

5.2.2. Battery balancing validation

To validate the balancing method, the initial SOC is set to 93%, 88%, 88%, and 80% for the four cells, respectively. In this scenario, the energy is balanced from C_1 to C_4. UDDS current profiles will be utilized to test the battery string and the balancing processes are performed according to the SOC-based balancing strategy simultaneously, as shown in Figure 18. The estimated SOC is denoted as rSOC, while the reference SOC is as eSOC in the figure.

Since the balancing process is based on SOC, the SOCs of the four cells should be first known. But these actual SOCs are not known to the SOC estimator. Initially, the SOC estimator assumes that the initial eSOC is 90% for all four cells. However, after a few sampling cycles of 50 to 100 s for example, the eSOC of each cell converges to the rSOC and the SOC differences of the cells can be observer by the balancing algorithm. With the eSOC obtained, the SOC-based balancing algorithms start to work efficiently, as shown in the figure. Eventually, the four cells are balanced according to the SOC in about 4000 s.

With the operation of the balancing procedures (as shown in Figure 18a), the SOC of C_4 and C_1 converge to the average SOC of cells, and finally the SOC of the four cells are almost the same, which could be considered as balanced. The voltage results of the balancing processes are also shown in Figure 18b. The voltages of the four cells are a lot different when the experiment starts, as shown in the first subplot of Figure 18b. After the balancing procedures, the voltages of the four cells converge to almost the same at the end of the experiment as shown in the second subplot of Figure 18b, which is another proof of the effectiveness of the balancing processes.

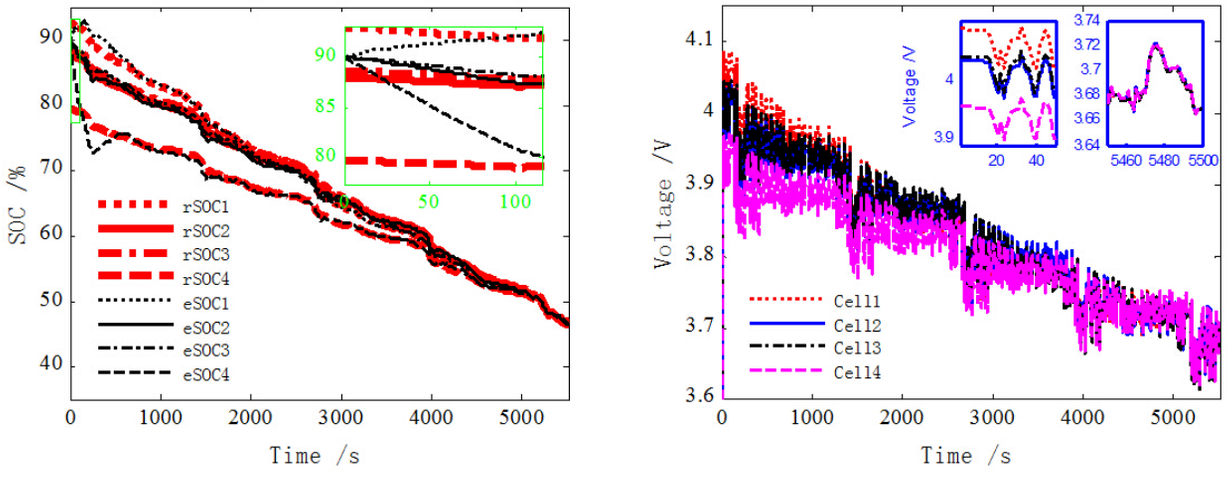

Figure 18. The results of battery balancing experiment: (a) SOC results for the balancing experiment. (b) Voltage results for the balancing experiment.

http://dx.doi.org/10.5772/61609

6. Conclusion

This chapter introduced advances in several popular BMS technologies, including battery modeling, battery state estimation, and battery balancing. Experimental workbench has been established to validate the aforementioned technologies. Several equivalent circuit battery models were first introduced and analyzed. Then based on it, the impedance model and the SOC estimation method were proposed. Several model-based SOC estimation methods were analyzed and the PI observer SOC estimation method was proposed. For the importance of balancing for battery strings in EDV applications, several existing balancing topologies were introduced and a novel cell to cell balancing topology was proposed. Finally, experimental tests were carried out to validate the effectiveness of the methods stated in this chapter. This chapter could be useful for BMS design and further study of technologies in this area.

Acknowledgements

The work was supported by the National Natural Science Foundation of China (51,405,374), the Postdoctoral Science Foundation of China (2014 M560763), the DOE/Chrysler under grant DE-EE0002720, and the China Scholarship Council (CSC) in part. The authors would like to thank Prof. Chris Mi of the University of Michigan, Dearborn for his kindly help.

Author details

Jun Xu* and Binggang Cao

*Address all correspondence to: xujun018@gmail.com

State Key Laboratory for Manufacturing Systems Engineering, School of Mechanical Engineering, Xi'an Jiaotong University, Xi'an, Shaanxi, China

References

[1] X. Wu, G. Guo, J. Xu, and B. Cao, "Application of Parallel Chaos Optimization Algorithm for Plug-in Hybrid Electric Vehicle Design," International Journal of Bifurcation and Chaos, vol. 24, 2014.

[2] X. Wu, B. Cao, X. Li, J. Xu, and X. Ren, "Component sizing optimization of plug-in hybrid electric vehicles," Applied Energy, vol. 88, pp. 799–804, 2010.

[3] B. Wang, J. Xu, B. Cao, and X. Zhou, "A novel multimode hybrid energy storage system and its energy management strategy for electric vehicles," Journal of Power Sources, vol. 281, pp. 432–443, 2015.

[4] B. Wang, J. Xu, and B. Cao, "Design of a novel hybrid power for EV," in Transportation Electrification Asia-Pacific (ITEC Asia-Pacific), 2014 IEEE Conference and Expo, 2014, pp. 1–5.

[5] Z. Chen, C. C. Mi, R. Xiong, J. Xu, and C. You, "Energy management of a power-split plug-in hybrid electric vehicle based on genetic algorithm and quadratic programming," Journal of Power Sources, vol. 248, pp. 416–426, 2014.

[6] Z. Chen, C. C. Mi, Y. Fu, J. Xu, and X. Gong, "Online Battery State of Health Estimation Based on Genetic Algorithm for Electric and Hybrid Vehicle Applications," Journal of Power Sources, vol. 240, pp. 184–192, 2013.

[7] Z. Chen, C. Mi, J. Xu, X. Gong, and C. You, "Energy Management for a Power-Split Plug-in Hybrid Electric Vehicle Based on Dynamic Programming and Neural Networks," Vehicular Technology, IEEE Transactions on, 2013.

[8] G. L. Plett, "Extended Kalman filtering for battery management systems of LiPB-based HEV battery packs: Part 2. Modeling and identification," Journal of Power Sources, vol. 134, pp. 262–276, 2004.

[9] V. H. Johnson, "Battery performance models in ADVISOR," Journal of Power Sources, vol. 110, pp. 321–329, 2002.

[10] H. He, R. Xiong, and J. Fan, "Evaluation of Lithium-Ion Battery Equivalent Circuit Models for State of Charge Estimation by an Experimental Approach," Energies, vol. 4, pp. 582–598, 2011.

[11] K. M. Tsang, L. Sun., and W. L. Chan, "Identification and modeling of Lithium ion battery," Energy Conversion and Management, vol. 51, pp. 2857–2862, 2010.

[12] Y. H. Chiang, W. Y. Sean, and J. C. Ke, "Online estimation of internal resistance and open-circuit voltage of lithium-ion batteries in electric vehicles," Journal of Power Sources, vol. 196, pp. 3921–3932, 2011.

[13] H. He, R. Xiong, X. Zhang, F. Sun., and J. Fan, "State-of-Charge Estimation of the Lithium-Ion Battery Using an Adaptive Extended Kalman Filter Based on an Improved Thevenin Model," Vehicular Technology, IEEE Transactions on, vol. 60, pp. 1461–1469, 2011.

[14] V. H. Johnson, A. A. Pesaran, T. Sack, and S. America, "Temperature-dependent battery models for high-power lithium-ion batteries," presented at the 17th Annual Electric Vehicle Symposium, Montreal, Canada, 2000.

[15] M. Sitterly, W. Le Yi, G. G. Yin, and W. Caisheng, "Enhanced Identification of Battery Models for Real-Time Battery Management," Sustainable Energy, IEEE Transactions on, vol. 2, pp. 300–308, 2011.

[16] P. Mauracher and E. Karden, "Dynamic modeling of lead/acid batteries using impedance spectroscopy for parameter identification," Journal of Power Sources, vol. 67, pp. 69–84, 1997.

[17] S. Buller, E. Karden, D. Kok, and R. W. De Doncker, "Modeling the dynamic behavior of supercapacitors using impedance spectroscopy," Industry Applications, IEEE Transactions on, vol. 38, pp. 1622–1626, 2002.

[18] S. Buller, "Impedance-Based Simulation Models for Energy Storage Devices in Advanced Automotive Power Systems," dissertation, RWTH Aachen University, 2002.

[19] C. Min and G. A. Rincon-Mora, "Accurate electrical battery model capable of predicting runtime and I-V performance," Energy Conversion, IEEE Transactions on, vol. 21, pp. 504–511, 2006.

[20] J. Xu, C. C. Mi, B. Cao, and J. Cao, "A new method to estimate the state of charge of lithium-ion batteries based on the battery impedance model," Journal of Power Sources, vol. 233, pp. 277–284, 2013.

[21] E. Karden, S. Buller, and R. W. De Doncker, "A method for measurement and interpretation of impedance spectra for industrial batteries," Journal of Power Sources, vol. 85, pp. 72–78, 2000.

[22] I. Sadli, M. Urbain, M. Hinaje, J.-P. Martin, S. Raël, and B. Davat, "Contributions of fractional differentiation to the modeling of electric double layer capacitance," Energy Conversion and Management, vol. 51, pp. 2993–2999, 2010.

[23] J. R. McDonald, Impedance Spectroscopy: Emphasizing solid materials and systems: Wiley-Interscience, 1987.

[24] I. Petráš, Fractional-Order Nonlinear Systems: Modeling, Analysis and Simulation: Springer Verlag, 2011.

[25] C. A. Monje, Y. Q. Chen, B. M. Vinagre, D. Xue, and V. Feliu, Fractional-order systems and controls: fundamentals and applications: Springer, 2010.

[26] J. A. T. Machado and A. Galhano, "Fractional Dynamics: A Statistical Perspective," Journal of Computational and Nonlinear Dynamics, vol. 3, pp. 021,201–5, 2008.

[27] J. Xu, J. Cao, B. Cao, and Y. Li, "Fractional three-loop autopilot of air-to-air missile with parameter optimization," Journal of Xi'an Jiaotong University, vol. 45, 2011.

[28] X. Yang, M. Liao, and J. Chen, "A Novel Approach to Processing Fractal Signals Using the Yang-Fourier Transforms," Procedia Engineering, vol. 29, pp. 2950–2954, 2012.

[29] J. Sabatier, M. Cugnet, S. Laruelle, S. Grugeon, B. Sahut, A. Oustaloup, et al., "A fractional order model for lead-acid battery crankability estimation," Communications in Nonlinear Science and Numerical Simulation, vol. 15, pp. 1308–1317, 2010.

[30] B. Pattipati, C. Sankavaram, and K. Pattipati, "System Identification and Estimation Framework for Pivotal Automotive Battery Management System Characteristics," Systems, Man, and Cybernetics, Part C: Applications and Reviews, IEEE Transactions on, vol. 41, pp. 869–884.

[31] K. Kutluay, Y. Cadirci, Y. S. Ozkazanc, and I. Cadirci, "A new online state-of-charge estimation and monitoring system for sealed lead-acid batteries in Telecommunication power supplies," Industrial Electronics, IEEE Transactions on, vol. 52, pp. 1315–1327, 2005.

[32] M. Charkhgard and M. Farrokhi, "State-of-Charge Estimation for Lithium-Ion Batteries Using Neural Networks and EKF," Industrial Electronics, IEEE Transactions on, vol. 57, pp. 4178–4187, 2010.

[33] L. Xu, J. Wang, and Q. Chen, "Kalman filtering state of charge estimation for battery management system based on a stochastic fuzzy neural network battery model," Energy Conversion and Management, vol. 53, pp. 33–39, 2012.

[34] Z. Zou, J. Xu, C. Mi, B. Cao, and Z. Chen, "Evaluation of Model Based State of Charge Estimation Methods for Lithium-Ion Batteries," Energies, vol. 7, pp. 5065–5082, 2014.

[35] J. Xu, B. Cao, Z. Chen, and Z. Zou, "An online state of charge estimation method with reduced prior battery testing information," International Journal of Electrical Power & Energy Systems, vol. 63, pp. 178–184, 2014.

[36] J. Xu, B. Cao, J. Cao, Z. Zou, C. C. Mi, and Z. Chen, "A Comparison Study of the Model Based SOC Estimation Methods for Lithium-Ion Batteries," in Vehicle Power and Propulsion Conference (VPPC), 2013 IEEE, 2013, pp. 1–5.

[37] X. Hu, F. Sun., and Y. Zou, "Estimation of State of Charge of a Lithium-Ion Battery Pack for Electric Vehicles Using an Adaptive Luenberger Observer," Energies, vol. 3, pp. 1586–1603, 2010.

[38] C. Lin, F. Zhang, H. Xue, and X. Lu, "Estimation of battery state of charge using H∞ observer," in Power Electronics and Motion Control Conference (IPEMC), 2012 7th International, 2012, pp. 422–428.

[39] F. Zhang, G. Liu, L. Fang, and H. Wang, "Estimation of Battery State of Charge with H∞ Observer: Applied to a Robot for Inspecting Power Transmission Lines," Industrial Electronics, IEEE Transactions on, pp. 1086–1095, 2012.

[40] G. L. Plett, "Extended Kalman filtering for battery management systems of LiPB-based HEV battery packs: Part 3. State and parameter estimation," Journal of Power Sources, vol. 134, pp. 277–292, 2004.

[41] G. L. Plett, "Extended Kalman filtering for battery management systems of LiPB-based HEV battery packs: Part 1. Background," Journal of Power Sources, vol. 134, pp. 252–261, 2004.

[42] I. S. Kim, "The novel state of charge estimation method for lithium battery using sliding mode observer," Journal of Power Sources, vol. 163, pp. 584–590, 2006.

[43] I. L.-S. Kim, "A Technique for Estimating the State of Health of Lithium Batteries Through a Dual-Sliding-Mode Observer," Power Electronics, IEEE Transactions on, vol. 25, pp. 1013–1022, 2010.

[44] C. R. Gould, C. M. Bingham, D. A. Stone, and P. Bentley, "New Battery Model and State-of-Health Determination Through Subspace Parameter Estimation and State-Observer Techniques," Vehicular Technology, IEEE Transactions on, vol. 58, pp. 3905–3916, 2009.

[45] D. Luenberger, "Observers for multivariable systems," Automatic Control, IEEE Transactions on, vol. 11, pp. 190–197, 1966.

[46] K. K. Busawon and P. Kabore, "Disturbance attenuation using proportional integral observers," International Journal of Control, vol. 74, pp. 618–627, 2012/07/18 2001.

[47] J. Xu, C. Mi, B. Cao, J. Deng, Z. Chen, and S. Li, "The State of Charge Estimation of Lithium-Ion Batteries Based on a Proportional Integral Observer "Vehicular Technology, IEEE Transactions on, vol. 63, pp. 1614–1621, 2014.

[48] C. Jeang-Lin, "Applying discrete-time proportional Integral observers for state and disturbance estimations," Automatic Control, IEEE Transactions on, vol. 51, pp. 814–818, 2006.

[49] D. SÖFFKER, T.-J. YU, and P. C. MÜLLERa, "State estimation of dynamical systems with nonlinearities by using proportional-integral observer," International Journal of Systems Science, vol. 26, pp. 1571–1582, 2012/12/20 1995.

[50] S. Beale and B. Shafai, "Robust control system design with a proportional integral observer," International Journal of Control, vol. 50, pp. 97–111, 2012/12/20 1989.

[51] E. Baker, H. Chon, and J. Keisler, "Battery technology for electric and hybrid vehicles: Expert views about prospects for advancement," Technological Forecasting and Social Change, vol. 77, pp. 1139–1146, 2010.

[52] K. C. Divya and J. Østergaard, "Battery energy storage technology for power systems - An overview," Electric Power Systems Research, vol. 79, pp. 511–520, 2009.

[53] L. Yuang-Shung and C. Ming-Wang, "Intelligent control battery equalization for series connected lithium-ion battery strings," Industrial Electronics, IEEE Transactions on, vol. 52, pp. 1297–1307, 2005.

[54] L. Yuang-Shung and C. Guo-Tian, "Quasi-Resonant Zero-Current-Switching Bidirectional Converter for Battery Equalization Applications," Power Electronics, IEEE Transactions on, vol. 21, pp. 1213–1224, 2006.

[55] L. A. Tolbert, P. Fang Zheng, T. Cunnyngham, and J. N. Chiasson, "Charge balance control schemes for cascade multilevel converter in hybrid electric vehicles," Industrial Electronics, IEEE Transactions on, vol. 49, pp. 1058–1064, 2002.

[56] L. Maharjan, S. Inoue, H. Akagi, and J. Asakura, "State-of-Charge (SOC)-Balancing Control of a Battery Energy Storage System Based on a Cascade PWM Converter," Power Electronics, IEEE Transactions on, vol. 24, pp. 1628–1636, 2009.

[57] P. Hong-Sun., K. Chong-Eun, K. Chol-Ho, M. Gun-Woo, and L. Joong-Hui, "A Modularized Charge Equalizer for an HEV Lithium-Ion Battery String," Industrial Electronics, IEEE Transactions on, vol. 56, pp. 1464–1476, 2009.

[58] A. C. Baughman and M. Ferdowsi, "Double-Tiered Switched-Capacitor Battery Charge Equalization Technique," Industrial Electronics, IEEE Transactions on, vol. 55, pp. 2277–2285, 2008.

[59] K. Nishijima, H. Sakamoto, and K. Harada, "A PWM controlled simple and high performance battery balancing system," in Power Electronics Specialists Conference, 2000. PESC 00. 2000 IEEE 31st Annual, 2000, pp. 517–520 vol.1.

[60] X. Aiguo, X. Shaojun, and L. Xiaobao, "Dynamic Voltage Equalization for Series-Connected Ultracapacitors in EV/HEV Applications," Vehicular Technology, IEEE Transactions on, vol. 58, pp. 3981–3987, 2009.

[61] N. H. Kutkut, "A modular nondissipative current diverter for EV battery charge equalization," in Applied Power Electronics Conference and Exposition, 1998. APEC '98. Conference Proceedings 1998., Thirteenth Annual, 1998, pp. 686–690 vol. 2.

[62] C. Karnjanapiboon, K. Jirasereeamornkul, and V. Monyakul, "High efficiency battery management system for serially connected battery string," in Industrial Electronics, 2009. ISIE 2009. IEEE International Symposium on, 2009, pp. 1504–1509.

[63] M. Einhorn, W. Guertlschmid, T. Blochberger, R. Kumpusch, R. Permann, F. Conte, et al., "A Current Equalization Method for Serially Connected Battery Cells Using a Single Power Converter for Each Cell," Vehicular Technology, IEEE Transactions on, vol. PP, pp. 1–1, 2011.

[64] W. Xuezhe and Z. Bing, "The research of vehicle power Li-ion battery pack balancing method," in The Ninth International Conference on Electronic Measurement & Instruments, 2009, pp. 2–498–2–502.

[65] M. Einhorn, W. Roessler, and J. Fleig, "Improved Performance of Serially Connected Li-Ion Batteries With Active Cell Balancing in Electric Vehicles," Vehicular Technology, IEEE Transactions on, vol. 60, pp. 2448–2457, 2011.

[66] W. XueZhe, Z. Xiaopeng, and H. Dai, "The application of flyback DC/DC converter in Li-ion batteries active balancing," in Vehicle Power and Propulsion Conference, 2009. VPPC '09. IEEE, 2009, pp. 1654–1656.

[67] N. H. Kutkut and D. M. Divan, "Dynamic equalization techniques for series battery stacks," in Telecommunications Energy Conference, 1996. INTELEC '96., 18th International, 1996, pp. 514–521.

[68] X. Zhang, P. Liu, and D. Wang, "The Design and Implementation of Smart Battery Management System Balance Technology," Journal of Convergence Information Technology, vol. 6, pp. 108–116, 2011.

[69] Y. Ye, K. W. E. Cheng, and Y. P. B. Yeung, "Zero-Current Switching Switched-Capacitor Zero-Voltage-Gap Automatic Equalization System for Series Battery String," Power Electronics, IEEE Transactions on, vol. 27, pp. 3234–3242.

[70] J. Xu, S. Li, C. Mi, Z. Chen, and B. Cao, "SOC Based Battery Cell Balancing with a Novel Topology and Reduced Component Count," Energies, vol. 6, pp. 2726–2740, 2013.

[71] P. B. T. Manual, "PNGV Battery Test Manual Revision 3," DOE/ID-10,597, February 2001.

IntechOpen